ACS chemical biology

Letters

pubs.acs.org/acschemicalbiology

Structure of *Enterococcus faecium* L,D-Transpeptidase Acylated by Ertapenem Provides Insight into the Inactivation Mechanism

Lauriane Lecoq,[†,‡,§] Vincent Dubée,[∥,⊥,#,¶] Sébastien Triboulet,[∥,⊥,#,¶] Catherine Bougault,[†,‡,§] Jean-Emmanuel Hugonnet,[∥,⊥,#] Michel Arthur,*[,∥,⊥,#] and Jean-Pierre Simorre*[,†,‡,§]

[†]CEA, Institut de Biologie Structurale Jean-Pierre Ebel, UMR 5075, Grenoble, France

[‡]CNRS, Institut de Biologie Structurale Jean-Pierre Ebel, UMR 5075, Grenoble, France

[§]Université Joseph Fourier−Grenoble 1, Institut de Biologie Structurale Jean-Pierre Ebel, UMR 5075, Grenoble, France

[∥]Centre de Recherche des Cordeliers, LRMA, Equipe 12, Université Pierre et Marie Curie−Paris 6, UMR S 872, Paris, France

[⊥]INSERM, U872, Paris, France

[#]Université Paris Descartes, Sorbonne Paris Cité, UMR S 872, Paris, France

Supporting Information

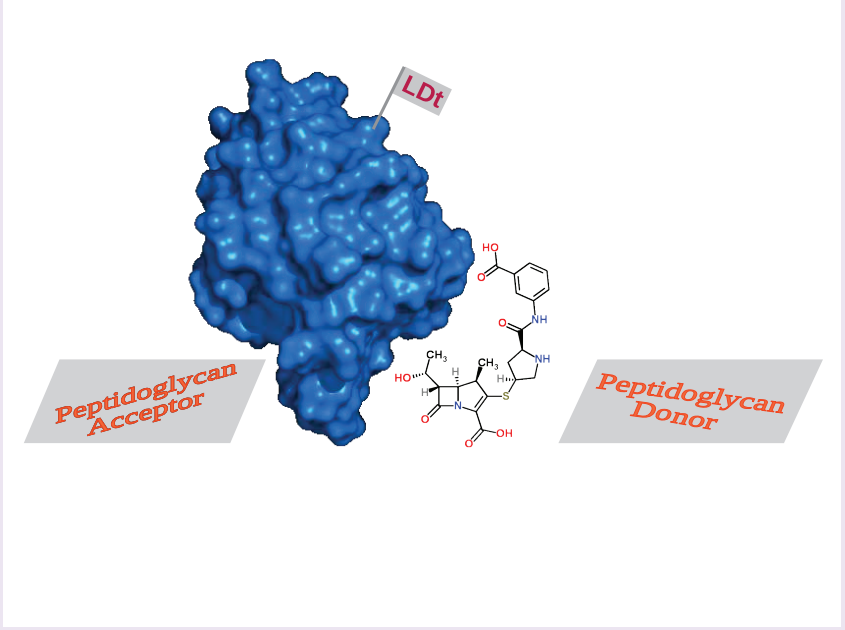

ABSTRACT: The maintenance of bacterial cell shape and integrity is largely attributed to peptidoglycan, a biopolymer highly cross-linked through D,D-transpeptidation. Peptidoglycan cross-linking is catalyzed by penicillin-binding proteins (PBPs) that are the essential target of β-lactam antibiotics. PBPs are functionally replaced by L,D-transpeptidases (Ldts) in ampicillin-resistant mutants of *Enterococcus faecium* and in wild-type *Mycobacterium tuberculosis*. Ldts are inhibited *in vivo* by a single class of β-lactams, the carbapenems, which act as a suicide substrate. We present here the first structure of a carbapenem-acylated L,D-transpeptidase, *E. faecium* Ldt_{fm} acylated by ertapenem, which revealed key contacts between the carbapenem core and residues of the catalytic cavity of the enzyme. Significant reorganization of the antibiotic conformation occurs upon enzyme acylation. These results, together with the analysis of protein-to-carbapenem proton transfers, provide new insights into the mechanism of Ldt acylation by carbapenems.

The peptidoglycan, an essential component of the bacterial cell wall, plays key roles in the maintenance of bacterial shape, in the resistance to osmotic pressure from the cytoplasm, and in the formation of daughter cells during cell division. As inhibition of peptidoglycan synthesis leads to bacterial cell lysis or death, its biosynthesis machinery is the favorite target of various antibiotics, including β-lactams. The latter drugs irreversibly inactivate D,D-transpeptidases, also referred to as penicillin-binding proteins (PBPs), that catalyze the last cross-linking step of peptidoglycan polymerization.[1] In *Enterococcus*

Received: March 5, 2013
Accepted: April 10, 2013
Published: April 10, 2013

dx.doi.org/10.1021/cb4001603 | *ACS Chem. Biol.* 2013, 8, 1140−1146

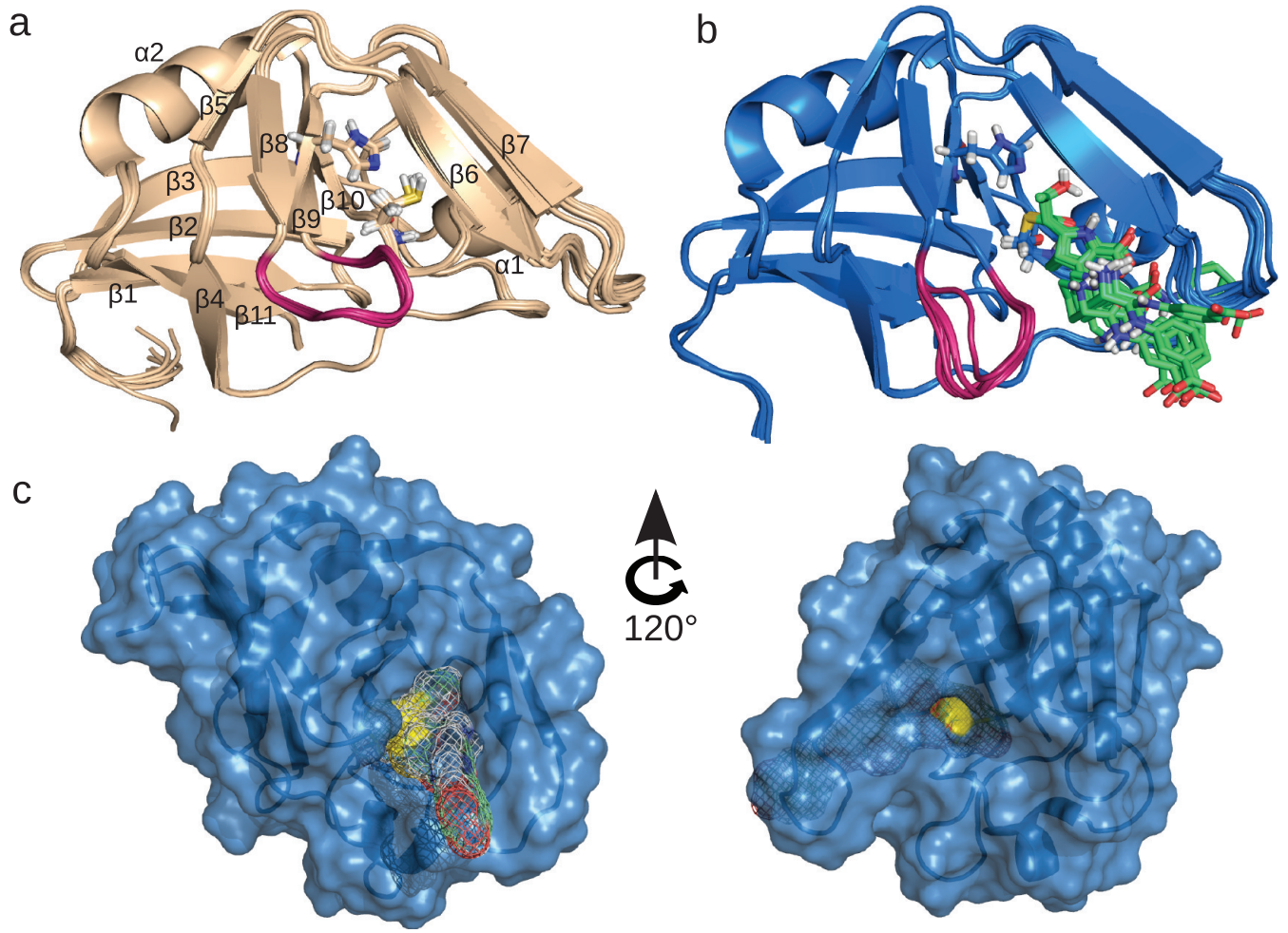

Figure 1. NMR structures of Ldt_{fm} apoenzyme and ertapenem−acylenzyme. (a) Ten structures of lowest energy of Ldt_{fm} apoenzyme. Catalytic residues His421 and Cys442 are shown as sticks. Secondary structure elements are numbered with their order of appearance in the sequence. (b) Ten structures of lowest energy of Ldt_{fm} acylated by ertapenem. His421 and Cys442−ertapenem (in green) are shown as sticks. Non−polar hydrogens of ertapenem are omitted for clarity. (c) Surface representation of the acylenzyme displayed in two orientations. Catalytic cysteine is colored in yellow and is accessible from two pockets highlighted in the left (Pocket 1) and right (Pocket 2) panels. Ertapenem is represented by a mesh surface in Pocket 1.

faecium, PBPs catalyze formation of 4 → 3 cross-links, which connect the carbonyl of D-Ala at the fourth position of a donor stem peptide to the amine of the D-iAsn side-chain at the third position of an acceptor stem peptide (D-Ala^4 → D-iAsn−L-Lys^3 cross-links). The transpeptidation reaction involves an intermediate esterification between the PBP active-site serine and the D-Ala^4 carbonyl after cleavage of the D-Ala^4−D-Ala^5 peptide bond of the donor stem peptide and release of D-Ala^5. The nucleophilic serine can also be acylated by β-lactams, which act as suicide substrates, form stable acylenzymes, and thereby irreversibly inactivate the PBPs. A new class of enzymes, the active-site cysteine L,D-transpeptidases (Ldts), was identified in β-lactam-resistant mutants of *E. faecium* selected *in vitro*[2] and in wild-type strains of *Mycobacterium tuberculosis*,[3] *Mycobacterium abscessus*,[4] and *Clostridium difficile*.[5] The L,D-transpeptidation pathway involves an essential D,D-carboxypeptidase that cleaves the D-Ala^4−D-Ala^5 bond of peptidoglycan precursors and generates the tetrapeptide stems used as the acyl donor in the cross-linking reaction.[6] In *E. faecium*, the Ldt forms L-Lys^3 → D-iAsn−L-Lys^3 cross-links following cleavage of the L-Lys^3−D-Ala^4 peptide bond of the donor stem tetrapeptide. Ldts are inactivated by a single β-lactam class, the carbapenems, which form a thioester bond with the active-site cysteine.[7−9] The carbapenem class includes four approved drugs, imipenem, ertapenem, doripenem, and meropenem, with similar structure and the same mode of action.[10]

The crystal structures of Ldts from *E. faecium* (Ldt_{fm}),[11] *Bacillus subtilis* (Ldt_{Bs}),[12] and *M. tuberculosis* (Ldt_{Mt2})[13] have been determined but crystallization of β-lactam-acylated forms of these enzymes has been unsuccessful. Recently, we have reported the NMR structure of Ldt_{Bs}, and we showed that acylation of this enzyme by imipenem induces substantial conformational flexibility in large regions of the protein.[14] The dynamics of the acylenzyme prevented the determination of a unique structure and the conformation of the drug in the active site could not be accurately obtained. To gain insight into the mechanism of the acylation of L,D-transpeptidases by β-lactams, we have solved the NMR structure of *E. faecium* Ldt_{fm} acylated by ertapenem. This first high-resolution structure of a carbapenem-acylated L,D-transpeptidase provides clues on antibiotic accessibility and antibiotic-enzyme stabilizing interactions and gives new insights into the mechanism of the acylation reaction.

dx.doi.org/10.1021/cb4001603 | *ACS Chem. Biol.* 2013, 8, 1140−1146

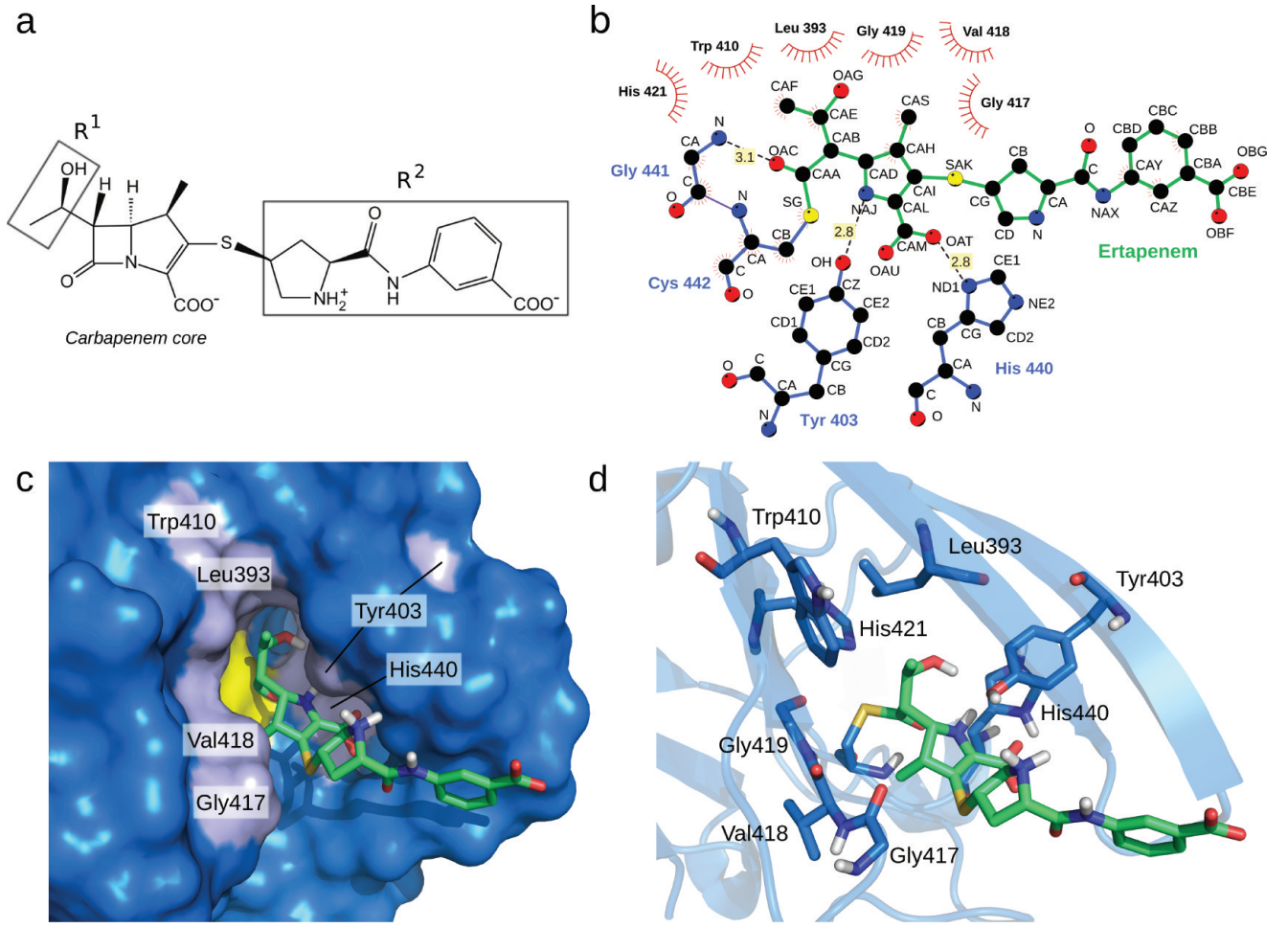

Figure 2. Stabilizing interactions between Ldt_{fm} and ertapenem in the acylenzyme. (a) Chemical structure of ertapenem comprising the carbapenem core and two side-chains. The R^1 hydroxyethyl side-chain is conserved among carbapenems, whereas R^2 is variable.[10] (b) Ligplot analysis[24] of ertapenem−Ldt_{fm} interactions. Leu393, Trp410, Gly417, Val418, Gly419, and catalytic His421 are involved in hydrophobic contacts. Tyr403, His440, and Gly441 are involved in hydrogen-bonding interactions with ertapenem. (c) Surface representation of the active site of Ldt_{fm} acylated by ertapenem. Protein residues in interaction with ertapenem are shown in light blue. Gly419 and His421 are hidden in this representation. (d) Cartoon representation of the acylenzyme active site. Residues in interaction with ertapenem are shown as sticks.

The X-ray structure of a fragment of Ldt_{fm} (residues 217 to 466) was solved in the absence of antibiotic.[11] This structure revealed the presence of two domains, an elongated N-terminal domain with a mixed $\alpha-\beta$ fold (residues 217 to 338), and a C-terminal catalytic domain (ErfK_YbiS_YhnG domain; Pfam PF03734). The NMR structural studies presented here were performed on the catalytic domain (residues 341 to 466), which displayed the same catalytic properties as the entire protein (Supplementary Table S1). Since the X-ray structure showed the presence of zinc and sulfate ions from crystallization conditions in the active site of this enzyme, the NMR solution structure of the catalytic domain of Ldt_{fm} was solved *de novo*. To refine the structure of the active site, protonation states of active-site residues were investigated by pH titration, using $^{1}H,^{13}C-HSQC$ and $^{1}H,^{15}N-SOFAST-HMQC$ spectra centered on aromatic and histidine imidazole rings, as previously described for the *B. subtilis* enzyme.[14] These analyses revealed a pK_a lower than 4.6 for conserved His421, which exists as the Nδ1 tautomer in the unprotonated form, and a pK_a superior to 9.9 for catalytic Cys442 (Supplementary Figure S1). These protonation states are similar to those found in the *B. subtilis* enzyme[14] and confirm the participation of Cys442 to a catalytic triad that comprises His421 and Asp422.[11]

The protonation states were included into the structure calculation protocol. The superposition of the 10 lowest energy NMR structures of Ldt_{fm} is shown in Figure 1a. The root-mean-square deviations (rmsds) for backbone and heavy atoms, as calculated from the 20 lowest energy structures, are 0.35 and 0.44 Å, respectively (see Supplementary Table S2 for further statistical analysis). These values indicate a remarkable convergence toward a well-defined structure. As expected, the NMR structure and the X-ray structure of the *E. faecium* catalytic domain[11] are very similar, with an rmsd of 1.03 Å over all backbone heavy atoms in common. The NMR structure is also similar (rmsd of 1.36 Å on backbone heavy atoms) to a recently published X-ray structure[13] of *M. tuberculosis*, Ldt_{Mt2} (Supplementary Figure S2), suggesting that the results of the present work extend to the L,D-transpeptidase of this pathogenic bacterium.

The NMR structure of the *E. faecium* catalytic domain acylated by ertapenem was solved after complete assignment of ^{1}H, ^{13}C, and ^{15}N resonances and collection of 3016 total NOE distance restraints including 27 drug−protein constraints. The 20 lowest energy NMR structures of the acylenzyme (see

dx.doi.org/10.1021/cb4001603 | *ACS Chem. Biol.* 2013, 8, 1140−1146

Figure 1b for the superposition of the 10 lowest energy structures) overlay with an rmsd of 0.23 and 0.59 Å for backbone and heavy atoms, respectively. A statistical analysis of 20 structures after water refinement is presented in Supplementary Table S2. A comparison of the structures from the apoenzyme (Figure 1a) and acylenzyme (Figure 1b) does not reveal any significant conformational rearrangement of the protein backbone (rmsd of 1.24 Å) with the exception of the loop connecting strands β8 and β9 (residues 413 to 418) highlighted in magenta.

As proposed by Biarrotte−Sorin et al.,[11] the catalytic cysteine of Ldt_{fm} is accessible from two sides of the protein. The first accessibility pocket (Pocket 1) is located between strand β6 and the loop connecting strands β8 and β9 (Figure 1c). The second accessibility pocket (Pocket 2) is located between strand β7 and a portion of the long loop connecting strands β9 to β10. The NMR structure of the acylenzyme reveals that ertapenem gets access to the cysteine from Pocket 1. This conclusion can be extended to other carbapenems based on NMR chemical shift perturbations observed with imipenem, doripenem, and meropenem (Supplementary Figure S3). Since carbapenems are thought to be structure analogues of the L-Lys^3−D-Ala^4 extremity of the acyl donor,[15] Pocket 1 is proposed as the binding site for the donor stem peptide during the peptidoglycan cross-linking reaction. Pocket 2 is the proposed binding site for the acceptor stem peptide, in agreement with the detection of a peptidoglycan fragment in the X-ray structure of *M. tuberculosis* Ldt_{Mt2}.[13]

The structure of Ldt_{fm} acylated by ertapenem reveals a good resolution of the 4-methyl-5-(2-oxoethyl)-4,5-dihydro-1*H*-pyrrole-2-carboxylate originating from the carbapenem core of the drug (Figure 2a) with an rmsd of 0.7 Å on all heavy atoms (Figure 1b). The hydroxyethyl side chain (R^1, Figure 2a), common to all carbapenems, is oriented toward the buried portion of Pocket 1 and is also very well-defined. In contrast, the bulky pyrrolidine-2-carboxylic acid-(3-carboxyphenyl)-amide R^2 side-chain of ertapenem (Figure 2a) is solvent-exposed and adopts multiple orientations in the final structure ensemble. The absence of detectable interactions between protein residues and the R^2 side-chain is in agreement with previous kinetics analyses that showed little impact of R^2 variations on the rate constants of the acylation reaction.[7]

The conformation of ertapenem in the acylenzyme is stabilized by a limited number of hydrogen bonds connecting the side chains of Tyr403 and His440 to the Δ^2-pyrroline ring of the carbapenem and the backbone amide of Gly441 to the carbonyl of the drug−Ldt_{fm} thioester group (Figure 2b−d). The ertapenem conformation is further stabilized by multiple hydrophobic interactions involving Leu393, Trp410, Gly417, Val418, and Gly419. Among these interactions, hydrophobic contacts between the antibiotic and residues 417−419 may be responsible for the conformational rearrangement of the loop connecting strands β8 and β9 upon Ldt_{fm} acylation by ertapenem (Figure 1).

Acylation of Ldt_{fm} by ertapenem leads to rupture of the bond between the nitrogen and the carbonyl carbon of the β-lactam ring (designated NAJ and CAA in Figure 2b, respectively). To obtain further insight into the modifications of the drug conformation associated with the rupture of the NAJ−CAA bond, we modeled ertapenem with a closed β-lactam ring, referred to as closed ertapenem, in the catalytic cavity of Ldt_{fm}. A structure of closed ertapenem was built using the PRODRG software.[16] The atoms of the Δ^2-pyrroline ring of the carbapenem from the closed ertapenem molecule were docked onto the corresponding atoms of the opened ertapenem present in the acylenzyme structure. The structure was refined with CNS[17] in a molecular dynamics simulation with explicit solvent using a distance restraint of 1.7 Å between the Sγ of catalytic Cys442 and the CAA carbonyl carbon of the β-lactam ring. Comparison of the drug conformation in the closed ertapenem model and in the acylenzyme indicated that rupture of the β-lactam CAA−NAJ bond increases the CAD−CAB−CAA angle by 60° and changes the CAA−NAJ distance from 1.3 to 2.8 Å (Figure 3). This structural rearrangement is

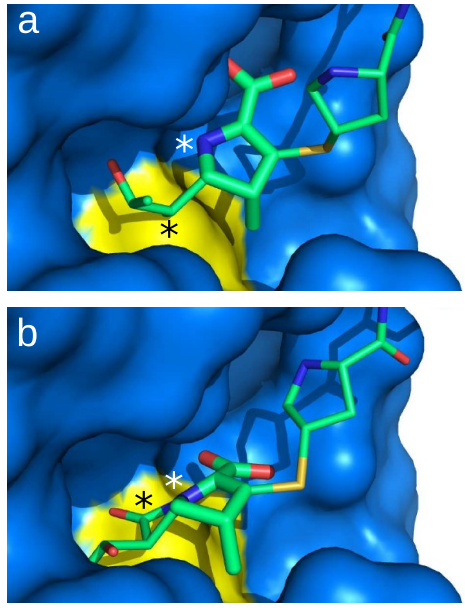

Figure 3. Carbapenem orientation in the open and closed conformations. (a) Surface representation of the acylenzyme. (b) Model of the enzyme with a closed β−lactam ring. The model is obtained by energy minimization of a closed ertapenem docked into the acylenzyme structure. A distance restraint between the CAA carbon of the β-lactam ring and the Sγ of Cys442 was used to obtain a structure in agreement with the intermediate oxyanion state. For clarity, the CAA carbon and the NAJ nitrogen atoms of the disrupted carbapenem bond are indicated with black and white stars, respectively.

required to generate the stabilizing drug−protein hydrogen-bond interactions in the acylenzyme (Figure 2b), including interactions between the pyrroline ring of ertapenem and Tyr403 and His440 residues of Ldt_{fm}, and interactions between the backbone amide of Gly441 and the thioester carbonyl of the drug−Ldt_{fm} covalent complex. This atomic reorganization disrupts the predicted hydrogen bond (2.9 Å) between the OAT atom of the carboxylate group of the antibiotic and the backbone amide of Gly441 (Supplementary Figure S4).

The rupture of the CAA−NAJ bond of the β-lactam ring is accompanied by a proton capture. The origin of this proton is unknown in L,D-transpeptidases. In the case of the *B. subtilis* enzyme, the Nε2 of the catalytic histidine was previously proposed to be the proton donor.[14] In the case of Ldt_{fm}, it is unlikely that the catalytic histidine plays this role since the distance between the β-lactam NAJ nitrogen and the catalytic His421 Nε2 is too large (5.9 Å) in the closed ertapenem model and even larger (6.9 ± 0.2 Å) in the acylenzyme (Figures 4b and c, respectively). The structure of the acylenzyme revealed

dx.doi.org/10.1021/cb4001603 | *ACS Chem. Biol.* 2013, 8, 1140−1146

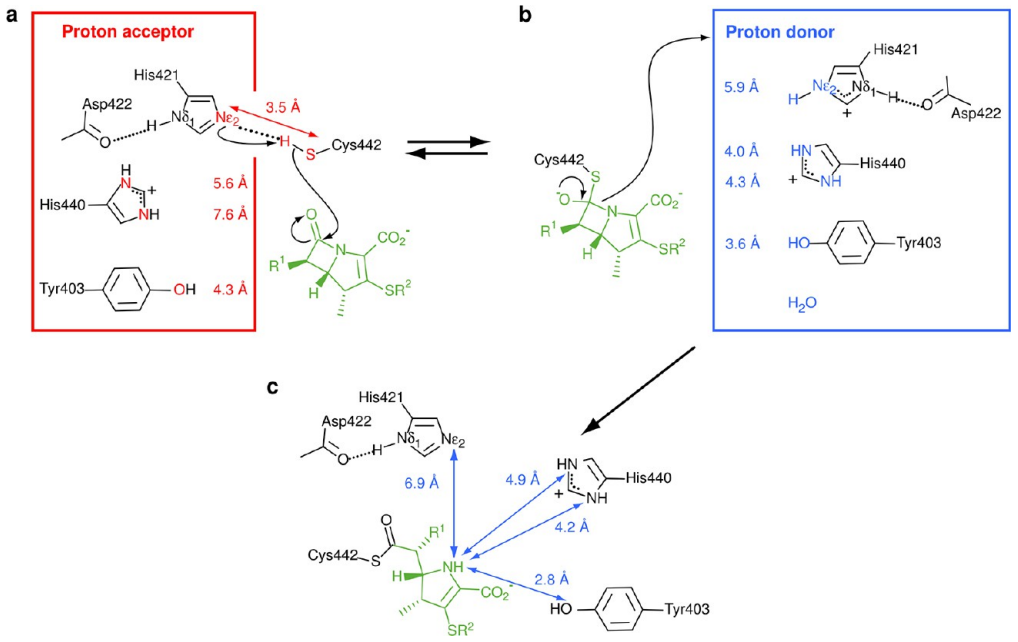

Figure 4. Proposed mechanism for the Ldt_{fm} acylation by ertapenem. Different structural states of Ldt_{fm} during the acylation reaction are schematically presented. (a) The nucleophilic attack of the β-lactam carbonyl by Cys442 requires activation into thiolate. The average distance (3.5 ± 0.3, 5.6 ± 0.7, 7.6 ± 0.6, and 4.3 ± 0.2 Å) between the catalytic cysteine Sγ and different proton acceptor candidates (His421 Nε2, His440 Nδ1, His440 Nε2, and Y403 O, respectively) as measured in 20 lowest energy structures of the apoenzyme are emphasized in red. The short Nε2−Sγ distance and the protonation state of the various residues lead to select His421 as the proton acceptor. (b) Structure of the oxyanion and putative origin of the proton captured by the NAJ nitrogen of the β-lactam ring upon rupture of the β-lactam CAA−NAJ bond. Distances in blue were measured in the closed ertapenem model between the NAJ nitrogen of the β-lactam ring and the heteroatom of the proton donor candidates. These data tend to exclude His421 as a reasonable proton donor. (c) Description of the protonation state of the previous proton donor candidates (His421 Nε2, His440 Nδ1, His440 Nε2, and Y403 O) as determined by NMR in the acylenzyme. Their distances to the NAJ atom of the opened ertapenem (6.9 ± 0.2, 4.2 ± 0.1, 4.9 ± 0.2, and 2.8 ± 0.1 Å, respectively) are reported in blue.

His440 and Tyr403 as potential proton donors, although a water molecule cannot be excluded. The NAJ nitrogen of the β-lactam ring may be protonated prior to or after conformational alteration of ertapenem. In the latter case, the hydroxyl of Tyr403 is an excellent candidate as it is appropriately located at 2.8 ± 0.1 Å from NAJ in the acylenzyme structure. In this scenario, acylation of Ldt_{fm} by ertapenem is expected to be, in part, thermodynamically driven by the hydrogen-bonding interactions generated by the conformational modification of the drug.

In conclusion, the high-resolution experimental and model structures proposed in the present study for the *E. faecium* L,D-transpeptidase apoenzyme, oxyanion intermediate and acylenzyme unravel a sequence of mechanistic events along the acylation reaction. The position of the carbapenem core has been assigned to one of the two pockets from which the Ldt_{fm} active site is accessible. This pocket is likely to accommodate the tetrapeptide donor stem during the cross-linking reaction with natural substrates. Future challenges include exploiting key features of the inhibition mechanism to assist drug design.

METHODS

Production and Purification of Ldt_{fm}. A $^{13}C,^{15}N$−labeled protein containing the catalytic domain (residues 341 to 466) of *E. faecium* Ldt was produced in *Escherichia coli* BL21 (DE3) cells harboring the pETTEVΩldt_{fm} plasmid in M9 minimal medium containing ^{13}C-glucose and $^{15}NH_4Cl$. The protein was purified by metal-affinity and size-exclusion chromatographies as previously described.[18] The purified protein was cleaved with a 6His-labeled TEV protease leaving three extra GHM residues at the N-terminal of the catalytic domain. The polyhistidine tag (MHHHHHHENLYFQ) and the TEV protease were removed using a NiNTA affinity resin.

NMR Spectroscopy. NMR samples were prepared in 100 mM sodium phosphate buffer, pH 6.4 containing 300 mM NaCl and 10% D_2O. Data for structure determination were collected on 0.9 mM $^{13}C,^{15}N$−labeled protein samples for both apo- and acylenzymes. To generate the latter, ertapenem (INVANZ) was incubated with Ldt_{fm} at a drug-to-protein molar ratio of 1. The NMR data were collected at 25 °C on 600 and 800 MHz Agilent Direct Drive spectrometers and on a 950 MHz Bruker Avance spectrometer. All spectrometers were equipped with triple resonance cryogenic probes. Backbone sequential resonances were assigned using 3D heteronuclear experiments. Three-dimensional ^{15}N−NOESY−HSQC (mixing time τ_m = 150 ms), 3D aliphatic ^{13}C−NOESY−HSQC (τ_m = 130 ms) in H_2O, and 3D aromatic ^{13}C−NOESY−HSQC (τ_m = 130 ms) in D_2O were recorded to extract distance restraints. Proton assignment of ertapenem when bound to Ldt_{fm} was performed using intramolecular NOEs measured with the 2D $^{13}C,^{15}N$-filtered NOESY experiment[19] recorded in D_2O (τ_m = 180 ms). According to these data (Supplementary Figure S5), the Δ^2-pyrroline isomer of the ertapenem was selected and introduced into the structure calculation protocol. This experiment was also used to obtain NOEs between unlabeled ertapenem and $^{13}C,^{15}N$−labeled Ldt_{fm} in the acylenzyme.

Structural Restraints. Secondary structure elements were identified by analysis of ^{13}C-chemical shifts, and phi/psi dihedral angular restraints were derived with TALOS+.[20] The automatic peak-picking and NOE assignment of the ^{15}N−NOESY−HSQC and aliphatic and aromatic ^{13}C−NOESY−HSQC spectra were performed using the iterative procedure of UNIO'10.[21] Peak-picking and assignment of the 2D $^{13}C,^{15}N$-filtered NOESY experiment were performed manually.

Structure Calculations. ARIA 2.3[22] was run with seven iterations calculating 100 structures and a last cycle including 1000 structures. The 20 structures with the lowest energy were subsequently refined

dx.doi.org/10.1021/cb4001603 | *ACS Chem. Biol.* 2013, 8, 1140−1146

with CNS[17] using explicit solvent in a molecular dynamics simulation. For the acylenzyme, the PRODRG webserver[16] was used to create the initial coordinates, topology, and parameter files of the ertapenem-bound cysteine, which was then introduced in the ARIA distribution. A similar procedure was used to create the closed ertapenem initial files that were introduced into CNS for energy minimization. No specific hydrogen bond restraint was introduced during the structure calculation. The CING webserver[23] was used for analysis of the structural ensembles and quality assessment of the structural data reported in Supplementary Table S2.

■ ASSOCIATED CONTENT

Supporting Information

Five figures and two tables, as well as additional references. This material is available free of charge via the Internet at http://pubs.acs.org.

Accession Codes

Coordinates of 20 structures of the Ldt_{fm} apoenzyme and ertapenem−acylenzyme have been deposited in the Protein Data Bank (PDB) under the accession codes 3ZG4 and 3ZGP, respectively. Chemical shifts and relaxation data have been deposited in the BioMagResBank (BMRB) under accession numbers 18900 and 18911.

■ AUTHOR INFORMATION

Corresponding Author

*E-mail: jean-pierre.simorre@ibs.fr (J.-P.S.); michel.arthur@crc.jussieu.fr (M.A.).

Author Contributions

¶These authors contributed equally to this work.

Notes

The authors declare no competing financial interest.

■ ACKNOWLEDGMENTS

This work was supported by the Agence National de la Recherche (ANR), Project CARBATUB (No. ANR 2011 BSV5 024 01) and the National Institute of Allergy and Infectious Diseases (Grants RO1 AI046626). Financial support of the French TGIR-RMN is acknowledged for conducting the research on the 950 MHz spectrometer of the ICSN Facility.

■ REFERENCES

(1) Zapun, A., Contreras-Martel, C., and Vernet, T. (2008) Penicillin-binding proteins and β-lactam resistance. *FEMS Microbiol. Rev. 32*, 361−385.

(2) Mainardi, J.-L., Fourgeaud, M., Hugonnet, J.-E., Dubost, L., Brouard, J.-P., Ouazzani, J., Rice, L. B., Gutmann, L., and Arthur, M. (2005) A novel peptidoglycan cross-linking enzyme for a β-lactam-resistant transpeptidation pathway. *J. Biol. Chem. 280*, 38146−38152.

(3) Lavollay, M., Arthur, M., Fourgeaud, M., Dubost, L., Marie, A., Veziris, N., Blanot, D., Gutmann, L., and Mainardi, J.-L. (2008) The peptidoglycan of stationary-phase *Mycobacterium tuberculosis* predominantly contains cross-links generated by L,D-transpeptidation. *J. Bacteriol. 190*, 4360−4366.

(4) Lavollay, M., Fourgeaud, M., Herrmann, J. L., Dubost, L., Marie, A., Gutmann, L., Arthur, M., and Mainardi, J.-L. (2011) The peptidoglycan of *Mycobacterium abscessus* is predominantly cross-linked by L,D-transpeptidases. *J. Bacteriol. 193*, 778−782.

(5) Peltier, J., Courtin, P., El Meouche, I., Lemee, L., Chapot-Chartier, M. P., and Pons, J. L. (2011) *Clostridium difficile* has an original peptidoglycan structure with a high level of *N*-acetylglucosamine deacetylation and mainly 3−3 cross-links. *J. Biol. Chem. 286*, 29053−29062.

(6) Sacco, E., Hugonnet, J.-E., Josseaume, N., Cremniter, J., Dubost, L., Marie, A., Patin, D., Blanot, D., Rice, L. B., Mainardi, J.-L., and Arthur, M. (2010) Activation of the L,D-transpeptidation peptidoglycan cross-linking pathway by a metallo-D,D-carboxypeptidase in *Enterococcus faecium*. *Mol. Microbiol. 75*, 874−885.

(7) Dubée, V., Arthur, M., Fief, H., Triboulet, S., Mainardi, J.-L., Gutmann, L., Sollogoub, M., Rice, L. B., Etheve-Quelquejeu, M., and Hugonnet, J. E. (2012) Kinetic analysis of *Enterococcus faecium* L,D-transpeptidase inactivation by carbapenems. *Antimicrob. Agents Chemother. 56*, 3409−3412.

(8) Dubée, V., Triboulet, S., Mainardi, J.-L., Etheve-Quelquejeu, M., Gutmann, L., Marie, A., Dubost, L., Hugonnet, J. E., and Arthur, M. (2012) Inactivation of *Mycobacterium tuberculosis* L,D-transpeptidase Ldt_{Mt1} by carbapenems and cephalosporins. *Antimicrob. Agents Chemother. 56*, 4189−4195.

(9) Mainardi, J.-L., Hugonnet, J.-E., Rusconi, F., Fourgeaud, M., Dubost, L., Moumi, A. N., Delfosse, V., Mayer, C., Gutmann, L., Rice, L. B., and Arthur, M. (2007) Unexpected inhibition of peptidoglycan L,D-transpeptidase from *Enterococcus faecium* by the β-lactam imipenem. *J. Biol. Chem. 282*, 30414−30422.

(10) Papp-Wallace, K. M., Endimiani, A., Taracila, M. A., and Bonomo, R. A. (2011) Carbapenems: past, present, and future. *Antimicrob. Agents Chemother. 55*, 4943−4960.

(11) Biarrotte-Sorin, S., Hugonnet, J.-E., Delfosse, V., Mainardi, J.-L., Gutmann, L., Arthur, M., and Mayer, C. (2006) Crystal structure of a novel β-lactam-insensitive peptidoglycan transpeptidase. *J. Mol. Biol. 359*, 533−538.

(12) Bielnicki, J., Devedjiev, Y., Derewenda, U., Dauter, Z., Joachimiak, A., and Derewenda, Z. S. (2005) *B. subtilis* YkuD protein at 2.0 Å resolution: insights into the structure and function of a novel, ubiquitous family of bacterial enzymes. *Proteins 62*, 144−151.

(13) Erdemli, S. B., Gupta, R., Bishai, W. R., Lamichhane, G., Amzel, L. M., and Bianchet, M. A. (2012) Targeting the cell wall of *Mycobacterium tuberculosis*: structure and mechanism of L,D-transpeptidase 2. *Structure 20*, 1−13.

(14) Lecoq, L., Bougault, C., Hugonnet, J.-E., Veckerlé, C., Pessey, O., Arthur, M., and Simorre, J.-P. (2012) Dynamics induced by β-lactam antibiotics in the active site of *Bacillus subtilis* L,D-transpeptidase. *Structure 20*, 850−861.

(15) Tipper, D., and Strominger, J. (1965) Mechanism of action of penicillins: a proposal based on their structural similarity to acyl-D-alanyl-D-alanine. *Proc. Natl. Acad. Sci. U.S.A. 54*, 1133−1141.

(16) Schüttelkopf, A. W., and van Aalten, D. M. F. (2004) PRODRG: a tool for high-throughput crystallography of protein−ligand complexes. *Acta Crystallogr., Sect. D: Biol. Crystallogr. 60*, 1355−1363.

(17) Brunger, A. T. (2007) Version 1.2 of the crystallography and NMR system. *Nat. Protoc. 2*, 2728−2733.

(18) Triboulet, S., Arthur, M., Mainardi, J.-L., Veckerlé, C., Dubée, V., Nguekam-Moumi, A., Gutmann, L., Rice, L. B., and Hugonnet, J.-E. (2011) Inactivation kinetics of a new target of β-lactam antibiotics. *J. Biol. Chem. 286*, 22777−22784.

(19) Wider, G., Weber, C., Traber, R., Widmer, H., and Wüthrich, K. (1990) Use of a double-half-filter in two-dimensional ^1H nuclear magnetic resonance studies of receptor-bound cyclosporin. *J. Am. Chem. Soc. 112*, 9015−9016.

(20) Shen, Y., Delaglio, F., Cornilescu, G., and Bax, A. (2009) TALOS+: a hybrid method for predicting protein backbone torsion angles from NMR chemical shift. *J. Biomol. NMR 44*, 213−223.

(21) Guerry, P., and Herrmann, T. (2011) Comprehensive automation for NMR structure determination of proteins, in *Methods in Molecular Biology*, pp 429−451, Humana Press, New York.

(22) Rieping, W., Habeck, M., Bardiaux, B., Bernard, A., Malliavin, T. E., and Nilges, M. (2007) ARIA2: automated NOE assignment and data integration in NMR structure calculation. *Bioinformatics 23*, 381−382.

(23) Doreleijers, J. F., Sousa da Silva, A. W., Krieger, E., Nabuurs, S. B., Spronk, C. A. E. M., Stevens, T. J., Vranken, W. F., Vriend, G., and Vuister, G. W. (2012) CING: an integrated residue-based structure validation program suite. *J. Biomol. NMR 54*, 267−283.

(24) Wallace, A., Laskowski, R., and Thornton, J. (1995) LIGPLOT: a program to generate schematic diagrams of protein−ligand interactions. *Protein Eng. 8*, 127−134.